General Cause of Sheath Instability Identified for Low Collisionality Plasmas in Devices with Secondary Electron Emission

M. D. Campanell, A. V. Khrabrov, and I. D. Kaganovich

Princeton Plasma Physics Laboratory, Princeton University, Princeton, New Jersey 08543, USA

(Received 11 October 2011; published 4 June 2012)

A condition for sheath instability due to secondary electron emission (SEE) is derived for low collisionality plasmas. When the SEE coefficient of the electrons bordering the depleted loss cone in energy space exceeds unity, the sheath potential is unstable to a negative perturbation. This result explains three different instability phenomena observed in Hall thruster simulations including a newly found state with spontaneous ~20 MHz oscillations. When instabilities occur, the SEE propagating between the walls becomes the dominant contribution to the particle flux, energy loss and axial transport.

DOI: 10.1103/PhysRevLett.108.235001 PACS numbers: 52.35.Qz, 52.40.Kh, 52.65.Rr

All laboratory plasmas inevitably contact other materials. The plasma-surface interaction (PSI) is a major factor limiting the performance of many devices. Modeling the PSI revolves around the sheaths [1] that form at the plasma-wall interfaces. Most models treat surfaces as a sink for charged particles and the resulting assumption of equal incident electron and ion fluxes in equilibrium determines sheath properties. However, depending on their impact energy and the target material, incident electrons may reflect off the surface or eject bound electrons from the surface [2]. Secondary electron emission (SEE) effects are critical for Hall thrusters (HT's) [3], tokamak divertors [4], Penning-type discharges [5], etc. For example, SEE reduces the strength of the sheath potential Φ that helps confine electrons, thereby enhancing power losses [6].

The magnitude of Φ is determined by the electron surface charge σ_e. A decrease (increase) of Φ raises (lowers) the number of electrons that can overcome the sheath and reach the surface. Without SEE, all electrons that reach the surface are absorbed. Fluctuations of Φ are self-canceled and the sheath is stable. But with SEE it is possible for the net differential conductivity of a sheath $dJ/d\Phi$ to be negative [7]. A sufficiently strong applied electron beam incident on a target in a plasma [8] can yield a negative differential conductivity because the emission induced by the beam is an increasing function of beam impact energy, which is a decreasing function of Φ. Sheath instability can also occur *naturally* in hot plasmas that induce strong SEE from the walls. Hall thruster simulations reveal sheath instabilities that abruptly alter the state of the plasma [9] and drive oscillations [10,11]. Sheath oscillations may considerably increase near-wall conductivity in HT's [10,12] and cause interference [13]. However, the precise causes and conditions for sheath instability are not yet quantified. Detecting such effects in HT's and other experiments is difficult among the many types of instability and oscillation that may occur. Therefore, it is important to develop the general theory of SEE-induced instability in more detail.

Computing $dJ/d\Phi$ requires detailed knowledge of the electron velocity distribution function (EVDF) [7]. In the high collisionality limit, emitted electrons thermalize in the plasma. One can then model the system adequately with a Maxwellian EVDF [14]. But in low collisionality plasmas, kinetic effects arise. For instance, simulations modeling the Princeton Plasma Physics Laboratory HT [15] show the bulk plasma is anisotropic with a strongly depleted loss cone, while SEE from each wall propagates across the plasma, impacting the other wall. These features create an irregular EVDF, making $dJ/d\Phi$ impossible to evaluate directly. But in this Letter, we show sheath instability in low collisionality plasmas depends in a simple way on the energies of electrons bordering the loss cone in energy space. A negative perturbation of Φ allows these "weakly confined electrons" (WCE's) to suddenly reach the wall. If and only if their energies *parallel* to the wall are large enough that their SEE coefficient γ_{WC} exceeds unity, this will reduce σ_e, which further lowers Φ, allowing more WCE's to reach the wall, etc.

To illustrate this concept, we explore various instabilities found in HT simulations. We use the 1D3V electrostatic direct implicit particle-in-cell code (EDIPIC) [16] to model a planar xenon plasma bounded by floating emitting walls, see Fig. 1(a). The main input variables are the uniform applied fields E_z and B_x, neutral gas density n_a, initial plasma density n_0, gap width H and turbulent collision frequency ν_{turb}. The plasma is assumed uniform in the y-z plane. The Poisson equation is solved using the direct implicit algorithm [17] to compute the plasma's self-generated field $E_x(x)$. Particle dynamics are governed by $E_x(x)$ and the $E \times B$ drift motion from the background fields. Electrons suffer Coulomb collisions and elastic collisions with neutrals. "Turbulent" collisions, introduced to produce anomalous conductivity, randomly scatter the y-z component of the velocity vector. This leads to displacement along E_z and an average y-z directed energy gain of $m_e V_{\mathrm{D}}^2$ per scatter, where $V_{\mathrm{D}} = E_z/B_x$ is the drift velocity. SEE is modeled with properties of boron nitride

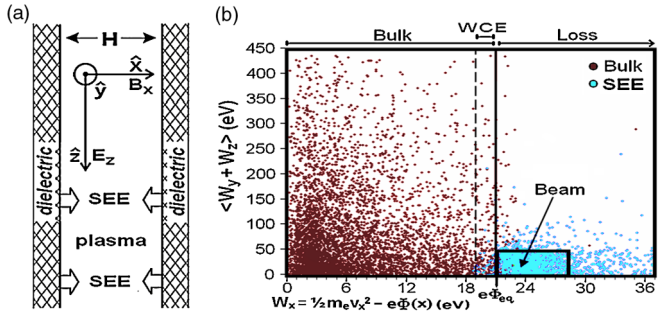

FIG. 1 (color online). (a) Model of the acceleration region of a Hall thruster. (b) Phase plot of bulk and secondary electrons at $t = 1000$ ns in the simulation detailed later in the Letter.

ceramics (BNC), a typical HT wall material. The average number of secondaries $\gamma(\varepsilon, \theta)$ produced by an electron with impact energy ε and angle relative to the normal θ is obtained from the model by Vaughan [18] in conjunction with experimental data [2]. EDIPIC was rigorously tested to reproduce experimental plasma behaviors. See Ref. [16] for more details regarding numerical algorithms, verification and past results.

Figure 1(b) shows a sample of electrons in energy space in a typical simulation. Electrons with $w_x < e\Phi$ are trapped in the potential well formed by the sheaths at the two walls. The average energy parallel to the walls $\langle w_\parallel \rangle = \langle w_z + w_y \rangle$ far exceeds $\langle w_x \rangle$ and $e\Phi$ because energy is gained from the electric field E_z while all electrons with $w_x > e\Phi$ quickly escape to the walls. The anisotropy and strongly depleted "loss region" seen in Fig. 1(b) are normal features of low collisionality plasmas, where collisions with neutrals are not frequent enough to maintain isotropy and replenish the loss cone. Secondaries are in the loss region because they are emitted from a wall (the "top" of the potential well) and have $w_x > e\Phi$ automatically. They are accelerated across the plasma by the sheath and reach the other wall. Most secondaries are emitted cold with small initial velocities. In transit across the plasma, they undergo drift motion with $w_\parallel$ varying from 0 to $2m_e V_D{}^2 = 45$ eV in Fig. 1(b). (Note, a small portion of the SEE consists of electrons that reflected elastically off the wall. These may have higher energies.)

The particle flux at each wall consists of several distinct components. Trapped "bulk" electrons can escape when their velocity vectors are scattered into the loss region by collisions with neutrals. The "collision-ejected electron" (CEE) flux is denoted Γ_{CE}. SEE from the opposite wall produces "beam" flux Γ_b. In equilibrium, because the two beams are equal and opposite by symmetry, it follows the incoming beam flux Γ_b and outgoing SEE flux at a wall are equal. The zero current condition becomes $\Gamma_{e,\mathrm{net}} = \Gamma_{e,\mathrm{in}} - \Gamma_{e,\mathrm{out}} = (\Gamma_{\mathrm{CE}} + \Gamma_b) - \Gamma_b = \Gamma_{\mathrm{CE}} = \Gamma_i$, where Γ_i is the ion flux. The equilibrium potential Φ_{eq} limits Γ_{CE} to maintain this balance. What determines Γ_b is that the SEE induced by the incident Γ_b and Γ_{CE} at a wall must combine to produce the outgoing SEE flux Γ_b. It is convenient to introduce partial SEE coefficients, where γ_X is the ratio of the secondary flux caused by flux component Γ_X, to Γ_X. The additional equilibrium condition becomes $\gamma_{\mathrm{CE}}\Gamma_{\mathrm{CE}} + \gamma_b\Gamma_b = \Gamma_b$, giving

$$\Gamma_b = \left(\frac{\gamma_{\mathrm{CE}}}{1 - \gamma_b}\right)\Gamma_{\mathrm{CE}}. \tag{1}$$

The net emission γ_{net} is the ratio of the total emitted flux to the incident electron flux at a wall, $(\gamma_{\mathrm{CE}}\Gamma_{\mathrm{CE}} + \gamma_b\Gamma_b)/(\Gamma_{\mathrm{CE}} + \Gamma_b)$. Using (1), we obtain

$$\gamma_{\mathrm{net}} = \gamma_{\mathrm{CE}}/(1 + \gamma_{\mathrm{CE}} - \gamma_b). \tag{2}$$

There is an additional flux component Γ_{WC} formed by WCE's with w_x slightly below $e\Phi$ that are nudged into the loss cone by fluctuations, such as from two-stream instability induced by the beams [19]. But the same fluctuations cause some beam electrons with w_x slightly above $e\Phi$ to become trapped in the potential well and not reach the other wall. These effects approximately cancel [15,19]. So when deriving the steady state flux balance equations, we could equivalently assume the beams penetrate fully across the plasma and ignore the WCE's. However, WCE's become critical during instability, as we will show.

From the structure of the system in Fig. 1(b), one can anticipate how it becomes unstable. For the case of a floating wall, sheath instability occurs if a negative perturbation of Φ causes reduction of σ_e, which further lowers Φ. Suppose a perturbation $-\Delta\Phi$ occurs. Γ_{WC} increases as previously trapped electrons with $e(\Phi - \Delta\Phi) < w_x < e\Phi$ reach the wall. $\Delta\Gamma_b = 0$ because secondaries emitted from the other wall are unaffected, as they have $w_x > e\Phi$. $\Delta\Gamma_{\mathrm{CE}}$, from the increase in size of the loss cone, is negligible because CEE density in the loss cone is very small in low collisionality. Bohm's criterion [1] implies Γ_i is independent of Φ. So overall, σ_e decreases if and only if $\gamma_{\mathrm{WC}} > 1$. More formally, in terms of the energy distribution in the plasma center $f_w(w_x, w_\parallel)$, stability depends on the sign of the expression,

$$\Delta\sigma_e \propto \int_0^\infty \int_{e(\Phi-\Delta\Phi)}^{e\Phi} f_w(w_x, w_\parallel)(1 - \gamma(\varepsilon, \theta))dw_x dw_\parallel, \tag{3}$$

where the kinetic impact energy is $\varepsilon = [w_x - e(\Phi - \Delta\Phi)] + w_\parallel$. For small $\Delta\Phi$, $\theta \to \pi/2$ for all $w_\parallel$ and (3) reduces to,

$$\Delta\sigma_e \propto \Delta\Phi \int_0^\infty f_w(e\Phi, w_\parallel)(1 - \gamma_{\mathrm{gr}}(w_\parallel))dw_\parallel, \tag{4}$$

where γ_{gr} is the SEE yield function at grazing incidence. For most materials in the energy range of interest ($\varepsilon <$ 400 eV) [18], including BNC [16], γ is a strongly increasing function of ε at all angles. The right-hand side of (4) is simply an integral over the parallel energies of electrons at the edge of the bulk, the WCE's. $\Delta\sigma_e < 0$ translates to

$\gamma_{WC} > 1$, where γ_{WC} is just an increasing function of parallel temperature $T_{\|}$.

There is a hidden assumption in (4); the sheath is not space-charge limited (SCL). If $\gamma_{net} > 1$, the negative charge layer formed by secondaries in the sheath creates a potential barrier that reflects some secondaries back to the wall so that γ_{net} (effective) saturates at a critical value $\gamma_{cr} < 1$, ($\gamma_{cr} \approx 0.983$ for xenon) [6]. In this case, any increase $\Delta\Gamma_{WC}$ in the WCE flux would only change the net flux by $(1 - \gamma_{cr})\Delta\Gamma_{WC}$, so that $\Delta\sigma_e > 0$. Thus the theory shows a SCL sheath is stable. However, provided $\gamma_b < 1$, true in general because secondaries are cold, it follows $\gamma_{net} < 1$ automatically via (2) no matter how hot the plasma is (i.e. how large γ_{CE} is). The beams ensure the formation of a classical non-SCL sheath in which the "$\gamma_{WC} > 1$ instability" can occur. This applies in general to bounded plasmas; the sheath-accelerated SEE passes between the walls unless collisionality is high enough to thermalize it. The SEE beam feedback (2) keeping γ_{net} below unity also occurs in cases where cold SEE from one wall returns to that wall after a time delay, such as by reflection off a stronger sheath in an asymmetric system, magnetic reflection in a mirror device [20] or by gyration in a grazing magnetic field such as in a tokamak [21].

We now show that three seemingly different instability phenomena observed in HT simulations all have the same underlying cause, $\gamma_{WC} > 1$. We present a run featuring all three effects for illustration. System parameters are in the ranges used to model contemporary experiments [15]. $E_z = 200$ V/cm, $B_x = 0.01$ T, $n_a = 10^{12}$ cm^{-3}, $n_0 = 1.1 \times 10^{11}$ cm^{-3}, $\nu_{turb} = 4.2 \times 10^6$ s^{-1}, and H=2.5cm. The initial state ($t = 0$) is a uniform Maxwellian EVDF with $T_e = 10$ eV in a cold ion background. The sheaths and a depleted loss cone form quickly over ~100 ns, so the theory developed here applies to the subsequent evolution of the plasma, see Fig. 2. EDIPIC records temporal data of the fluxes and partial SEE yields by component (CEE, WCE, beam). Throughout this run $\gamma_{CE} > 1$ but $\gamma_{net} < 1$ via Eq. (2) because $\gamma_b < 1$. Therefore, instability should occur if $\gamma_{WC} > 1$.

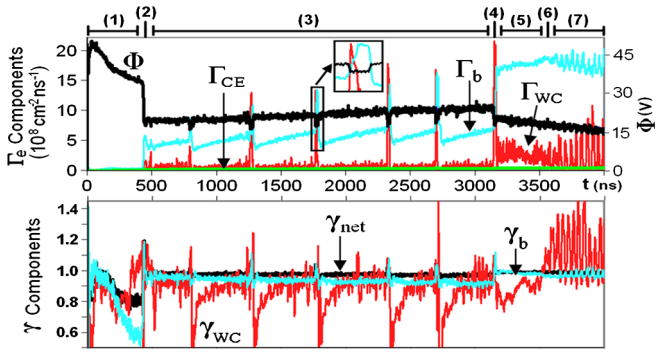

FIG. 2 (color online). Evolution of key parameters in the simulation. Formally, $\Phi \equiv |\Phi(x = H) - \Phi(x = H/2)|$. Also note $\gamma_{CE} \approx 2$ (out of range above).

Relaxation sheath oscillations (RSO's) are quasiperiodic instabilities appearing in interval 3 of Fig. 2. Typical oscillatory behavior of the *total* electron flux, average electron energy and potential in RSO's was first introduced in Ref. [11], but the precise cause of instability was unknown. Here, by tracking the flux components separately, one can see each period in interval 3 that the abrupt changes marking instability occur when γ_{WC} reaches unity. The plot of γ_{WC} appears noisy as the WCE flux in steady state is intrinsically fluctuation-driven, but it has been verified over dozens of simulations with RSO's that $\gamma_{WC} = 1$ is the critical point of instability. The RSO process can now be explained as follows. When γ_{WC} reaches unity, the sheaths become unstable. Φ rapidly drops while Γ_{WC} jumps (see the magnified box near $t = 1780$ ns). This causes a corresponding jump in the SEE outflux. Because $\gamma_b < 1$, when the intense SEE outflux reaches the opposite walls and Γ_b increases, there is a net absorption of electrons and Φ rises from its minimum Φ_{min} back to its initial value, Φ_{eq}. The potential increase traps some cold secondaries emitted during the drop into the WCE region of the EVDF ($e\Phi_{min} < w_x < e\Phi_{eq}$). This is why $\gamma_{WC} < 1$ after Φ restores and the plasma enters a stable interval. Gradually, the WCE's regain energy until γ_{WC} reaches 1 again. The process repeats periodically.

Estimating when $\gamma_{WC} < 1$ in terms of system parameters can predict what HT regimes are stable. The bulk EVDF in this HT model can be approximated as bi-Maxwellian with temperatures $T_{\|} = T_z$ and T_x, where T_z scales as $E_z{}^2\nu_{turb}$ [15]. As γ_{WC} depends on the parallel energies of electrons at the bulk edge, see (4), instability occurs if T_z exceeds a critical value. We ran simulations over a range of E_z and ν_{turb}, with all else constant. For given E_z, RSO's arose whenever ν_{turb} exceeded a critical value and vice versa, as expected. Note that the stability theory is not restricted to HT's because the requirement is on the temperature itself parallel to a surface $T_{\|}$, not the type of device or particular heating mechanism.

Another type of instability in HT simulations occurs at point 2 in Fig. 2 (also see Fig. 3). The plasma evolves smoothly from its initial state until at $t = 430$ ns, Φ abruptly drops by ~half and the total electron flux becomes ~10 times larger afterward. In contrast to RSO's, Φ does not return to its initial value and the plasma permanently changes. In Ref. [9] this type of instability was thought to be caused by the sinusoidal modulation of the phase of beam drift energy in its flight time τ_{flight} between the walls, since the beam energy changes (see γ_b in Fig. 3). Because the emission velocity is assumed small, τ_{flight} is roughly the same for all secondaries ($\tau_{flight} \sim 1/v_{x,avg} \sim \Phi^{-1/2}$). Thus the beam is coherent and its impact energy becomes, where $\omega_c = eB_x/m_e$,

$$w_b \approx m_e V_D{}^2[1 - \cos[\omega_c \tau_{flight}(\Phi)]]. \quad (5)$$

A decrease of Φ increases τ_{flight}, changing the beam's phase of $E \times B$ energy upon impact. Reference [9] argues if

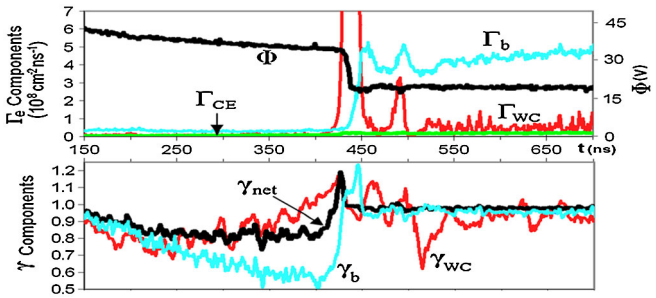

FIG. 3 (color online). Closer view of the "beam instability" (point 2 of Fig. 2).

$d\gamma_b/d\Phi < 0$, the SEE outflux increases so that $\Delta\sigma_e < 0$ and instability occurs. However, the derivation overlooked the effect of WCE's on the system when Φ decreases. The number of WCE's that reach the walls during a potential drop far exceeds the initial beam fluxes (compare the Γ_{WC} peak in Fig. 3 to Γ_b before instability). So the WCE influence on stability still dominates if $\gamma_{WC} < 1$. Also, the beam phase theory implies Φ would be unstable in both directions, but potential jumps are never observed in simulations. Only drops occur, as predicted in this new theory.

Focusing on the WCE's reveals that "beam instabilities" always occur when γ_{WC} crosses unity, see Fig. 3. Thus, the beam phase changes as a result of a "$\gamma_{WC} > 1$ instability." To see why γ_b changes, consider equilibrium condition (1). From (5), w_b can range from 0 to $2m_eV_D{}^2$. In runs with $E_z = 200$ V/cm and $B_x = 0.01$ T, $2m_eV_D{}^2 = 45$ eV. For BNC where $\gamma(\varepsilon,\theta) \approx \gamma(\varepsilon) \approx 0.17\varepsilon^{1/2}$ (ε in eV) [2], γ_b could vary in principle from zero to unity. But surprisingly, all simulations with instabilities tended to have γ_b near unity. The fact that γ_b jumps from 0.55 to 0.96 after instability in Fig. 3 cannot be a coincidence. Explaining the origin of this behavior is critical because Γ_b becomes very large compared to Γ_{CE} via (1) as $\gamma_b \to 1$. The $E \times B$ drift motion of secondaries increases axial transport and adds to the energy loss in HT's [3]. When Γ_b jumps by a factor of $\sim$15 after the transition in Fig. 3, the total power loss and axial conductivity increase dramatically ($\sim$ 10 times). So this effect has major implications on HT efficiency.

Similarly to RSO's, when γ_{WC} reaches unity in Fig. 3, Φ drops, causing a jump in Γ_{WC} (at both walls). When the intense SEE crosses the plasma, Γ_b jumps and Φ is no longer decreasing. At this point, Γ_{WC} is small again, Γ_{CE} is weakly changed, but Γ_b is still very large. For any Γ_b, Γ_{CE}, and γ_{CE}, there is a γ_b such that equilibrium condition (1) holds. After instability, the beams recharge the walls only to the extent needed for a self-consistent equilibrium to establish between the CEE flux, beam flux and SEE flux. Since there is ample freedom in γ_b via drift rotation (5) the system is able to remain in a state with very intense Γ_b simply by restoring to a potential in which γ_b becomes close to 1. In general, as in Fig. 3, this potential is lower than before the instability. However, if γ_b is already near unity, Φ must restore close to its initial value. This explains why further instabilities after point 2 in Fig. 2 became quasiperiodic RSO's. γ_b changes only at a slow average rate in interval 3. Then another beam instability occurs at point 4, bringing γ_b closer to 1 again.

A newly discovered regime appears in this run when γ_{WC} crosses unity at point 6 in Fig. 2. In the other two cases discussed, γ_{WC} reaches unity from below, instability occurs and the system restores to a stable state with $\gamma_{WC} < 1$. But in interval 7, γ_{WC} is well above unity, so the plasma is perpetually unstable and a new type of oscillation occurs, see Fig. 4. Starting at $t = 3692$ ns, Φ drops slightly, causing Γ_{WC} to increase. Γ_b then increases after a delay $\tau_{flight} \approx 10$ ns when the secondaries emitted during the drop cross the plasma. Because $\gamma_b < 1$, the excess beam flux recharges the walls to the initial potential. The fundamental difference between this regime and RSO's is that here, γ_{WC} still exceeds unity even when Φ restores, so instability quickly reoccurs. This is a true oscillation unlike the periodic instabilities in RSO's. The characteristic frequency is $\sim$10 times higher because there is no stable interval in this regime.

Overall, we have shown that sheath stability in low collisionality plasmas with SEE depends entirely on the energies of the weakly confined electrons. Simulated Hall thruster plasmas were always stable and smoothly evolving in time intervals when $\gamma_{WC} < 1$. Several phenomena may occur when $\gamma_{WC} > 1$ including (a) the transition to a high loss regime with intense SEE beam flux, (b) quasiperiodic instabilities (RSO's), and (c) high frequency oscillations of Γ_{WC}. Interestingly, studying instability also gave insight into equilibrium behavior of HT currents. An instability naturally leads to a stable state where the SEE becomes the dominant wall flux, causing enormous increases in power loss and axial conductivity.

We presented results from HT simulations, but the instability concept is broader because the condition $\gamma_{WC} > 1$ is unrelated to the background $E \times B$ field. The results apply in general to weakly collisional plasmas with strong SEE. When the temperature $T_{\|}$ parallel to a surface is sufficiently high, the sheath potential is unstable to a negative perturbation.

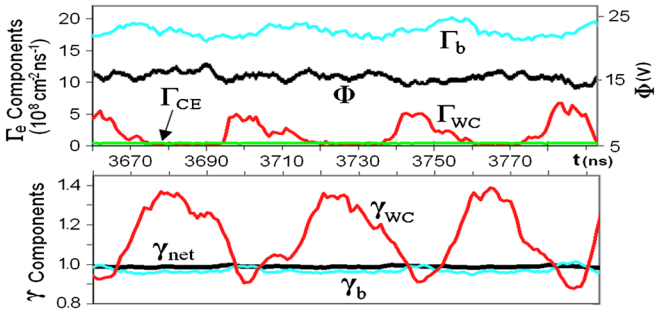

FIG. 4 (color online). High frequency WCE oscillations (from Fig. 2, interval 7).

The authors are indebted to Dmytro Sydorenko, the developer of the EDIPIC code. This work was supported by the U.S. Department of Energy.

[1] K. -U. Riemann, J. Phys. D **24**, 493 (1991).
[2] A. Dunaevsky, Y. Raitses, and N. J. Fisch, Phys. Plasmas **10**, 2574 (2003).
[3] Y. Raitses, I. D. Kaganovich, A. Khrabrov, D. Sydorenko, N. J. Fisch, and A. Smolyakov, IEEE Trans. Plasma Sci. **39**, 995 (2011).
[4] S. Takamura, N. Ohno, M. Y. Ye, and T. Kuwabara, Contrib. Plasma Phys. **44**, 126 (2004).
[5] M. O. Aboelfotoh and J. A. Lorenzen, J. Appl. Phys. **48**, 4754 (1977).
[6] G. D. Hobbs and J. A. Wesson, Plasma Phys. **9**, 85 (1967).
[7] A. I. Morozov, Sov. J. Plasma Phys. **17**, 393 (1991).
[8] M. C. Griskey and R. L. Stenzel, Phys. Rev. Lett. **82**, 556 (1999).
[9] D. Sydorenko, A. Smolyakov, I. Kaganovich, and Y. Raitses, Phys. Plasmas **15**, 053506 (2008).
[10] F. Taccogna, S. Longo, M. Capitelli, and R. Schneider, Appl. Phys. Lett. **94**, 251502 (2009).
[11] D. Sydorenko, I. Kaganovich, Y. Raitses, and A. Smolyakov, Phys. Rev. Lett. **103**, 14 (2009).
[12] D. Yu, H. Li, and Z. Wu, Phys. Plasmas **14**, 064505 (2007).
[13] A. A. Litvak, Y. Raitses, and N. J. Fisch, Phys. Plasmas **11**, 1701 (2004).
[14] E. Ahedo, Phys. Plasmas **9**, 4340 (2002).
[15] I. D. Kaganovich, Y. Raitses, D. Sydorenko, and A. Smolyakov, Phys. Plasmas **14**, 057104 (2007).
[16] D. Sydorenko, Ph.D. thesis, U. of Saskatchewan, 2006.
[17] A. B. Langdon, B. I. Cohen, and A. Friedman, J. Comput. Phys. **51**, 107 (1983).
[18] J. R. M. Vaughan, IEEE Trans. Electron Devices **36**, 1963 (1989).
[19] D. Sydorenko, A. Smolyakov, I. Kaganovich, and Y. Raitses, Phys. Plasmas **14**, 013508 (2007).
[20] D. D. Ryutov, Fusion Sci. Technol. **47**, 148 (2005).
[21] S. Mizoshita, K. Shiraishi, N. Ohno, and S. Takamura, J. Nucl. Mater. **220–222**, 488 (1995).